







# Investigation of the Consistency Between Anisotropic Covariance Structure of the Local Gravity Signal and the Mass Density through the Patch-wise Least Squares Collocation in Gravity Field Modelling

(Selected Paper in the 8<sup>th</sup> ISPRS Geospatial Conference 2025, University of Tehran, Iran)

Sabah Ramouz<sup>1</sup> , Abdolreza Safari<sup>2</sup> , Mirko Reguzzoni<sup>3</sup> , and Lorenzo Rossi<sup>4</sup> 

1. Corresponding author, School of Surveying and Geospatial Engineering, Faculty of Engineering, University of Tehran, Iran. E-mail: [sabah.ramouz@ut.ac.ir](mailto:sabah.ramouz@ut.ac.ir)
2. School of Surveying and Geospatial Information Engineering, Faculty of Engineering, University of Tehran, Iran. E-mail: [asafari@ut.ac.ir](mailto:asafari@ut.ac.ir)
3. Department of Civil and Environmental Engineering (DICA), Politecnico di Milano, Milano, Italy. E-mail: [mirko.reguzzoni@polimi.it](mailto:mirko.reguzzoni@polimi.it)
4. Department of Civil and Environmental Engineering (DICA), Politecnico di Milano, Milano, Italy. E-mail: [lorenzo1.rossi@polimi.it](mailto:lorenzo1.rossi@polimi.it)

## Article Info

**Article type:**  
Research Article

**Article history:**

Received 2026-01-16  
Received in revised form 2026-05-01  
Accepted 2026-05-02  
Available online 2026-06-02

**Keywords:**

Patch-wise Least Squares Collocation,  
Remove-Compute-Restore,  
Local gravity field,  
Anisotropic covariance,  
Density anomaly.

## ABSTRACT

Patch-wise Least Squares Collocation is introduced as a localized and optimized form of the conventional Least Squares Collocation method. It aims to mitigate the negative effects of the stationarity assumption and to better recover the high-frequency components of local signals. Conceptually, patching refers to the spatial subdivision of the study area into smaller regions, where local modelling within each patch reduces the error arising from assuming global stationarity. In Patch-wise Least Squares Collocation, inspired by the Remote-Compute-Restore concept, patching is performed by considering the spatial-spectral correspondence of the field. Accordingly, the patch dimensions are selected in proportion to the degree or order used in removing the long-wavelength components of the field.

Patch-wise Least Squares Collocation can also be implemented using anisotropic covariance functions. In this approach, for each patch, an anisotropic covariance is determined based on the observations within that region. Assuming local stationarity and anisotropy, the field is modelled in each patch independently of observations in other patches, and the estimated signal is represented as a vector of patch-wise estimates. In this regard, optimising the patching strategy in Patch-wise Least Squares Collocation is an attempt to enhance the gravity modelling. To do this, available geological and geophysical information could be useful resources to be used. As an initial try in this field, the anisotropic covariance derived from gravity anomalies and density anomalies are computed in a region in north-western of Iran. Results in this case study shows a considerable correlation between the anisotropy direction and elongation of these two covariances.

**Cite this article:** Ramouz, S., Safari, A., Reguzzoni, M., & Rossi, L. (2025). Investigation of the Consistency Between Anisotropic Covariance Structure of the Local Gravity Signal and the Mass Density in the Patch-Wise Gravity Field Modelling, *Earth Observation and Geomatics Engineering*, Volume 9, Issue 2, Pages 111-117. <http://doi.org/10.22059/eoge.2026.409762.1198>



## 1. Introduction

Patch-wise Least Squares Collocation (PLSC) is introduced as a localized and optimized form of the conventional Least Squares Collocation (LSC) method (Kamali et al., under review). This approach is inspired from two earlier attempts. First was introduced by Moritz (1980) when presented the idea of stepwise LSC as a solution for areas with a large number of observations, aimed at reducing the computational burden of matrix inversions. In this approach, by dividing observations into two vectors, not only the computational load is reduced, but also allows the incorporation of additional data to improve the initial estimate. In the case of presence of additional observations dataset, the second dataset could be in the same locations and different time (time-variable), or different locations inside the region or in another region.

Later, researchers at the Politecnico di Milano extended stepwise LSC to multistep LSC in order to process the massive volume of GOCE gravity gradients for spherical harmonic modeling (Reguzzoni and Tselfes, 2009). Their approach was consisted of estimating a regular grid of gravity data at satellite altitude. Then estimating spherical harmonic coefficients using collocation method. To reduce the computational load of inverting covariance matrices, in the first stage they restricted the estimation of each grid node to the local observations in its neighbourhood, rather than the entire dataset. So, they used multi-step because their method applied collocation repeatedly in successive stages, not just once, to recover high frequencies cut by the Wiener Filter and to fit within the space-wise approach.

PLSC also aims to mitigate the negative effects of the stationarity assumption and to better recover the high-frequency components of local signals. Conceptually, patching refers to the spatial subdivision of the study area into smaller regions, where local modelling within each patch reduces the error arising from assuming global stationarity.

In PLSC, inspired by the Remote-Compute-Restore (RCR) concept (Sanso & Sideris, 2013), patching is performed by considering the spatial-spectral correspondence of the field. Accordingly, the patch dimensions are selected in proportion to the degree and order used in removing the long-wavelength components of the field (Kamali et al., under review).

An important extension of PLSC is the use of anisotropic covariance functions, in which the covariance parameters vary with direction. This approach was first explored in the context of LSC by Darbeheshti (2009). In the PLSC setting, an anisotropic covariance is estimated independently for each patch using only the gravity observations inside that patch. Assuming local stationarity and local anisotropy, the final gravity signal is assembled from the set of patch-wise estimates. In recent studies, patching has been implemented using equiareal patches whose sizes match the spectral bandwidth of the removed global gravity signal (Kamali et al., under review).

The present study builds upon this framework with two objectives. First, we compute patch-wise anisotropic covariance models derived from a laterally varying density field, and integrate them into the PLSC formulation. Second, we investigate the relationship between the anisotropy and elongation of covariance functions estimated from terrestrial gravity anomalies and those derived from the lateral density variations. A case study in north-western Iran is used to illustrate the methodology. Section 2 discusses the PLSC formulation and the implementation of anisotropic covariance modeling. Section 3 presents the case study and analyzes the correlation between gravity-derived and density-derived anisotropy and elongation. Section 4 summarizes the main findings and outlines directions for future research.

## 2. Methodology

By introducing the observation after removing the systematic effect  $z = (l - \mathbf{ax})$ , observation equation can be rewritten in vector form as

$$Z = L - \mathbf{Ax} = \mathbf{Bs} + E. \quad (1)$$

Where  $L = [l_1 l_2 \dots l_n]^T$ ,  $E = [e_1 e_2 \dots e_n]^T$  are vector of the observations and their errors in a region. Now, by consideration of an auto-covariance matrix  $\bar{\mathbf{C}}_{LL} = \mathbf{C}_{LL} + \mathbf{C}_{EE}$  as the sum of the covariance matrix of the observations and that of the errors, the Wiener-Kolmogorov relation for the vector of the  $m$  sampling points ( $S = s_1, s_2, \dots, s_m$ ) in the region becomes

$$\hat{\mathbf{S}} = \mathbf{C}_{SL} \bar{\mathbf{C}}_{LL}^{-1} Z. \quad (2)$$

This equation in matrix form will be

$$\begin{bmatrix} \hat{s}_1 \\ \hat{s}_2 \\ \vdots \\ \hat{s}_m \end{bmatrix} = \begin{bmatrix} C_{s_1 l_1} & C_{s_1 l_2} & \dots & C_{s_1 l_n} \\ C_{s_2 l_1} & C_{s_2 l_2} & \dots & C_{s_2 l_n} \\ \vdots & \vdots & \ddots & \vdots \\ C_{s_m l_1} & C_{s_m l_2} & \dots & C_{s_m l_n} \end{bmatrix} \times \begin{bmatrix} \bar{C}_{l_1 l_1} & \bar{C}(l_1, l_2) & \dots & \bar{C}_{l_1 l_n} \\ \bar{C}_{l_2 l_1} & \bar{C}(l_2, l_2) & \dots & \bar{C}_{l_2 l_n} \\ \vdots & \vdots & \ddots & \vdots \\ \bar{C}_{l_n l_1} & \bar{C}_{l_n l_2} & \dots & \bar{C}_{l_n l_n} \end{bmatrix}^{-1} \begin{bmatrix} z_1 \\ z_2 \\ \vdots \\ z_n \end{bmatrix}. \quad (3)$$

Initially, LSC is applied considering stationarity assumption. This means that the covariance function that is used to compute the values of auto and cross-covariance matrices are solely affected by the distance between the points in the gravity field, without dependence to the location of the points or the direction between them. In local gravity modeling, stationarity assumption does not hold everywhere. Darbeheshti (2009) borrowed the nonstationary covariance function defined by Paciorek and Schervish (2006) and applied it to execute LSC without stationarity assumption. Paciorek and Schervish (2006) presented nonstationary covariance in the generalization of the relation of Higdon (1999). This covariance is defined as

$$C^N(P, Q) = \|\Sigma_P\|^{1/4} \|\Sigma_Q\|^{1/4} \left\| \frac{\Sigma_P + \Sigma_Q}{2} \right\|^{-1/2} F(C_0, D(P, Q)) \quad (4)$$

and is a function of the variance  $C_0$ , the Mahalanobis distance between the pair of observations  $D(P, Q)$ , and the kernel matrix  $\Sigma$  at the two points  $P$  and  $Q$ . The Mahalanobis distance between the pair of observations  $D(P, Q)$  is expressed by relation

$$D(P, Q) = \sqrt{[x_Q - x_P \quad y_Q - y_P] \left( \frac{\Sigma_P + \Sigma_Q}{2} \right)^{-1} \begin{bmatrix} x_Q - x_P \\ y_Q - y_P \end{bmatrix}} \quad (5)$$

and the kernel matrix  $\Sigma$  at each point is given in the form

$$\Sigma = \begin{bmatrix} \cos \theta & -\sin \theta \\ \sin \theta & \cos \theta \end{bmatrix} \begin{bmatrix} b^2 & 0 \\ 0 & a^2 \end{bmatrix} \begin{bmatrix} \cos \theta & \sin \theta \\ -\sin \theta & \cos \theta \end{bmatrix} \quad (6)$$

in which  $\theta$  is the anisotropy angle, and  $a$  and  $b$  are the major and minor axes of the anisotropy ellipse at that point. According to Figure 1, the kernel of Higdon (1999), which is the basis of the definition of the non-stationary covariance, is formulated with the geometry of the ellipse (major and minor axes) and its orientation in the plane (anisotropy angle).

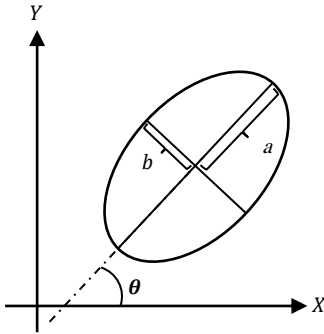


Figure 1: Geometry of the ellipse used in modeling the kernel matrix of Higdon (1999).

It should be noted that in this method, the vector of observations is in the form of a regular grid of gravity measurements, and the W-K Equation (3) is written based on the covariance between points  $j$  and  $i$ . This method, although it considers non-stationarity for the whole field and defines the field theoretically everywhere non-stationary and anisotropic, but in practice, in computing the parameters  $a$  and  $b$  the variations and differences of these covariance parameters of adjacent points can be so large that the continuity and smoothness of the field function is violated.

In fact, the expression  $\|\Sigma_P\|^{1/4} \|\Sigma_Q\|^{1/4} \left\| \frac{\Sigma_P + \Sigma_Q}{2} \right\|^{-1/2}$  in Equation (4) filters the behaviour of the non-stationary covariance. For this reason, Paciorek and Schervish (2006) added a scale parameter  $\tau$  to Equation (6) to empirically control the behaviour of the determined covariance.

Another way to mitigate the effect of stationarity assumption in LSC is spatially localization. PLSC make use of spatial patching and spatial-spectral correspondence - by

taking inspiration from the RCR theory - in the same time to employ localization. In PLSC, the covariance function could be either isotropic or anisotropic (Kamali et al., under review). Here, we think about the anisotropic covariance.

In this way, the case study is divided into a set of  $t$  patches, and in each patch, based on the observations located in it, an anisotropic covariance is computed. With this idea, by assuming stationarity and anisotropy of the field in each patch  $i$  and using anisotropic covariance for that patch, the modelling of the field in patch  $i$  is carried out independently of the observations of other patches, and the estimated signal  $s$  also becomes a vector of estimated signals  $s_i$  for  $i = 1, 2, \dots, t$ . As a result, for estimating the covariance parameters and producing the kernel matrix of each patch, there will be no need for parameter  $\tau$ . With the kernel matrix being constant in each patch, the Mahalanobis distance in Equation (5) becomes

$$D(P, Q) = \sqrt{[x_Q - x_P \quad y_Q - y_P] \Sigma^{-1} \begin{bmatrix} x_Q - x_P \\ y_Q - y_P \end{bmatrix}} \quad (7)$$

and the anisotropic covariance of that patch is defined in the form

$$C^{SA}(P, Q) = F(C_0, D(P, Q)). \quad (8)$$

In this case, PLSC extend Equation (2) into

$$\begin{bmatrix} \hat{S}_1 \\ \hat{S}_2 \\ \vdots \\ \hat{S}_m \end{bmatrix} = \begin{bmatrix} \mathbf{C}_{S_1 L_1} & 0 & \dots & 0 \\ 0 & \mathbf{C}_{S_2 L_2} & \dots & 0 \\ \vdots & \vdots & \ddots & \vdots \\ 0 & 0 & \dots & \mathbf{C}_{S_m L_m} \end{bmatrix} \times \begin{bmatrix} \bar{\mathbf{C}}_{L_1 L_1} & 0 & \dots & 0 \\ 0 & \bar{\mathbf{C}}_{L_2 L_2} & \dots & 0 \\ \vdots & \vdots & \ddots & \vdots \\ 0 & 0 & \dots & \bar{\mathbf{C}}_{L_m L_m} \end{bmatrix}^{-1} \begin{bmatrix} \hat{Z}_1 \\ \hat{Z}_2 \\ \vdots \\ \hat{Z}_m \end{bmatrix}. \quad (9)$$

Here,  $\hat{S}_i$  is the estimated signal vector in patch  $i$ . In PLSC, modeling within each patch is independent of observations in other patches, making the auto-covariance and cross-covariance matrices block-diagonal. This substantially reduces computation compared to Darbehesti (2009) approach.

In Equation (9),  $\mathbf{C}_{S_i L_i}$  and  $\bar{\mathbf{C}}_{L_i L_i}$  are matrices of auto-covariance between observations  $L_i$  and cross-covariance between observations  $L_i$  and unknown signal  $s_i$  in patch  $i$  as

$$\bar{\mathbf{C}}_{L_i L_i} = \begin{bmatrix} \bar{C}_{l_i^1 l_i^1} & \bar{C}_{l_i^1 l_i^2} & \dots & \bar{C}_{l_i^1 l_i^{m_i}} \\ \bar{C}_{l_i^2 l_i^1} & \bar{C}_{l_i^2 l_i^2} & \dots & \bar{C}_{l_i^2 l_i^{m_i}} \\ \vdots & \vdots & \ddots & \vdots \\ \bar{C}_{l_i^{n_i} l_i^1} & \bar{C}_{l_i^{n_i} l_i^2} & \dots & \bar{C}_{l_i^{n_i} l_i^{m_i}} \end{bmatrix} \quad (10)$$

and

$$C_{s_i L_i} = \begin{bmatrix} C_{s_i^1 l_i^1} & C_{s_i^1 l_i^2} & \dots & C_{s_i^1 l_i^{m_i}} \\ C_{s_i^2 l_i^1} & C_{s_i^2 l_i^2} & \dots & C_{s_i^2 l_i^{m_i}} \\ \vdots & \vdots & \ddots & \vdots \\ C_{s_i^{n_i} l_i^1} & C_{s_i^{n_i} l_i^2} & \dots & C_{s_i^{n_i} l_i^{m_i}} \end{bmatrix}. \quad (11)$$

In Equation (10),  $\bar{C}_{l_i^j l_i^k} = C_{l_i^j l_i^k} + C_{e_i^j e_i^k}$  is the sum of covariances between observations at points  $j$  and  $k$  and errors between them and in Equation (11),  $C_{s_i^j l_i^k}$  is the covariance between observation at point  $k$  and unknown signal at point  $j$  in patch  $i$ . Consequently, localization in PLSC improves the recovery of high-frequency components in gravity field modelling.

### 3. Case Study and Results

As shown in Figure 2a, the study area R1 in north-western Iran with a network of terrestrial gravity observations by  $\sim 5$  arc-minute is chosen (Ramouz et al., 2020). These observations after remove the normal gravity and Free-air reduction are converted to free-air gravity anomaly ( $\Delta g_{FA}^{obs}$ ). To execute gravity modelling it is required to transform these free-air gravity anomalies into reduced gravity anomalies

$$\Delta g_{res} = \Delta g_{FA}^{obs} - \Delta g_N^{GGM} - \Delta g_{RTM}^{TC}. \quad (12)$$

$\Delta g_N^{GGM}$  is the effect of global gravity signal up to degree and order (d/o)  $N$  equals to 360, which is quantified using a global gravity model (GGM).  $\Delta g_{RTM}^{TC}$  is also the effect of short wavelengths of the field caused by topographic correction, which is calculated by the *RTM* method (Forsberg, 1984). In fact, *RTM* is a method used for topographic correction in the Molodensky paradigm. Gravity observations of this case study are reduced using EIGEN-6C4 for global (Förste et al, 2014) and SRTM digital elevation model (Farr et al, 2007) for topographic effects.

Here patching of the area is handled based on the spatial spherical resolution  $\psi_{min}$ , related to the maximum d/o  $N$  of the spherical harmonic expansion of the removed GGM. If the surface of the sphere is divided into equal patches, spherical harmonics of (d/o)  $N$  produce  $(N + 1)^2$  number of coefficients. Then the size of these patches is equal to

$$A = \frac{4\pi R^2}{(N+1)^2} \quad (13)$$

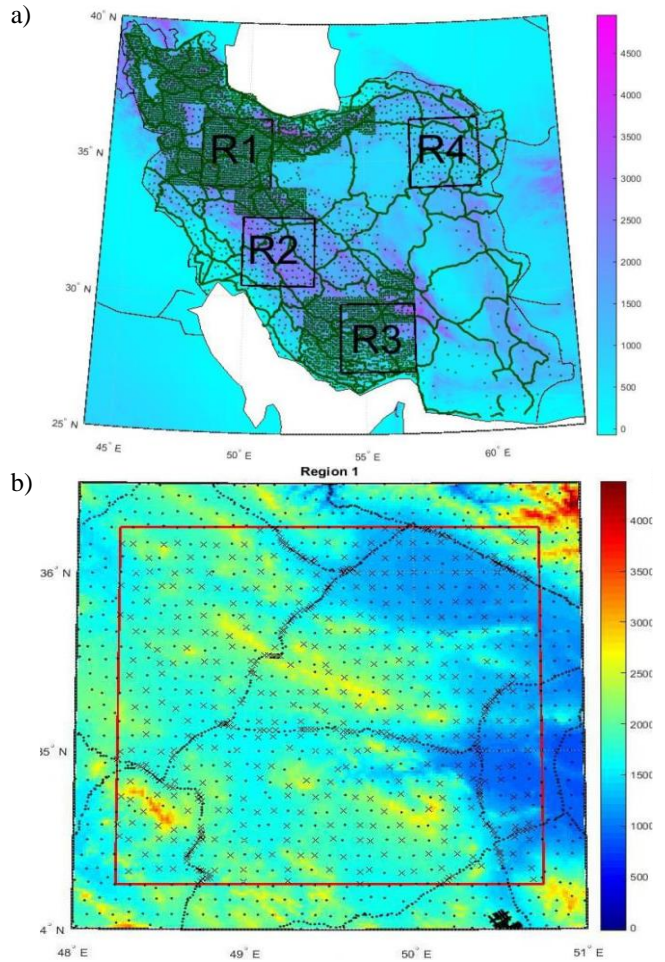
where  $R$  is the mean Earth radius. The diameter of the spherical cap, which lies down in area  $A$ , can be assumed as spherical resolution (Barthelmes, 2013)

$$\psi_{min} = 4 \sin^{-1} \left( \frac{1}{N+1} \right). \quad (14)$$

According to Eq. (14), in this case study, spherical harmonic expansion up to d/o  $N = 360$  has a resolution of  $\psi_{min} \approx 70 \text{ km}$ . By removing the global effect up to d/o  $N$  from observations, the effect of all the components outside of the area with the size of  $\psi_{min}$  will be ignored in the residual signal. This means that only local components including

topography and/or geological features contribute to the residual signal. With respect to this property of RCR (i.e., spectral localization), the covariance of a patch with the size of  $\psi_{min}$  will be independent from outer observation. So, this case study is divided into 16 equal patches (Figure 2b) of about 70 km ( $\sim 44'$ ).

To determine anisotropic covariance of Eq. 8, there are several covariance functions such as Gaussian, Exponential, or 3rd order Markov function. As a new approach, Kamali et al. (under review) introduced Covariance Estimation by Cross-validation (CEC) algorithm in patch-wise anisotropic covariance determination (Figure 2b).



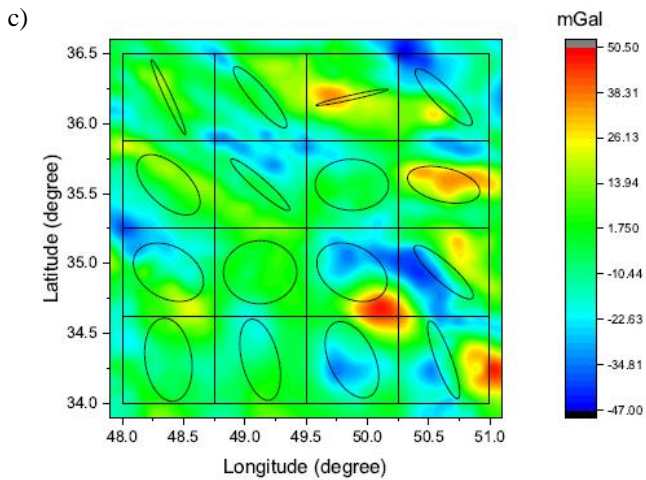


Figure 2. a) Location of the R1 study area in Iran with topography in background (Ramouz et al., 2020), b) Distribution of the gravimetry observations on R1 region consist of 3<sup>rd</sup> degree gravity network (with 5 arc-minute spacing) and gravity measurement along 1<sup>st</sup> leveling network of Iran (Ramouz et al., 2020), c) gravity-derived patch-wise anisotropic covariances of the R1 area with the background of residual gravity field distribution (Kamali et al., under review).

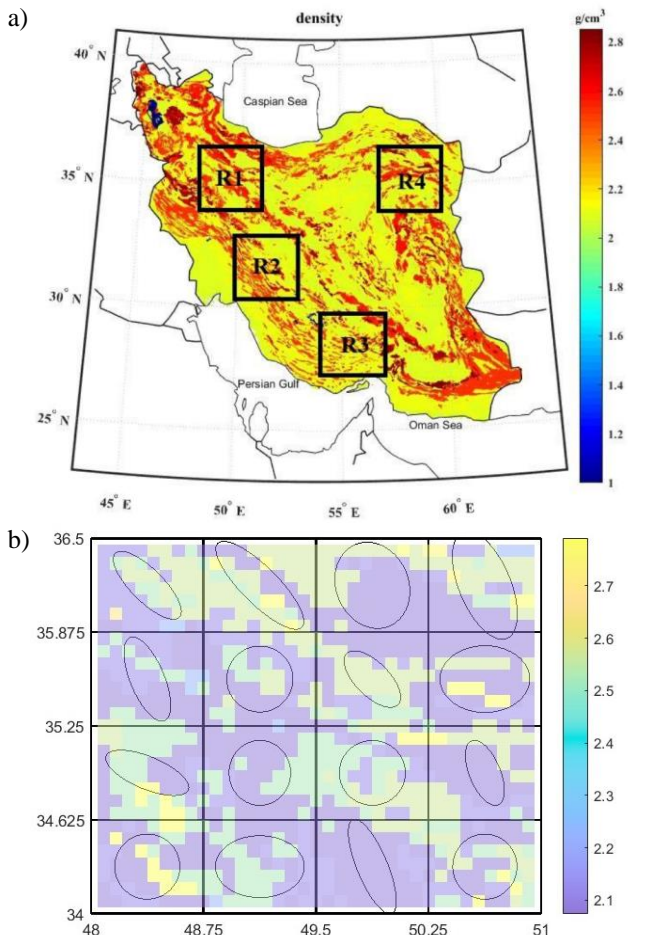


Figure 3. a) UNB\_TopoDensT\_2v01 model (5 arc-minute) over Iran (Ghasemi et al., 2020), b) density-derived patch-wise anisotropic covariances of the R1 area based on UNB\_TopoDensT\_2v01. Background is UNB\_TopoDensT\_2v01.

In order to evaluate the concept of patch-wise independency of gravity field in PLSC, the global topographical density UNB\_TopoDensT\_2v01 model with 5 arc-minute resolution is employed (Sheng et al., 2019). This 2D model is derived from Global Lithology Model (Hartmann and Moosdorf, 2012) through assigning surface density values to lithologies using Tenzer et al, 2011 geological database. Whereas higher resolution of UNB\_TopoDensT\_2v01 (30 arc-second) is also available, 5 arc-minute resolution is employed, Because, 30 arc-second resolution is solely reliable where the input maps to GLiM have similar resolution (Sheng et al., 2019).

5 arc-minute laterally varying topographical density in Iran is shown in Figure 3a (Ghasemi et al., 2023) and for case study of this work (R1) in the background of Figure 3b. Figure 3b also includes laterally-varying density-derived patch-wise anisotropic covariances in R1. These covariances which are scaled to fit the size of patches, are determined by fitting to an empirical anisotropic covariances in each patch. The empirical covariances are

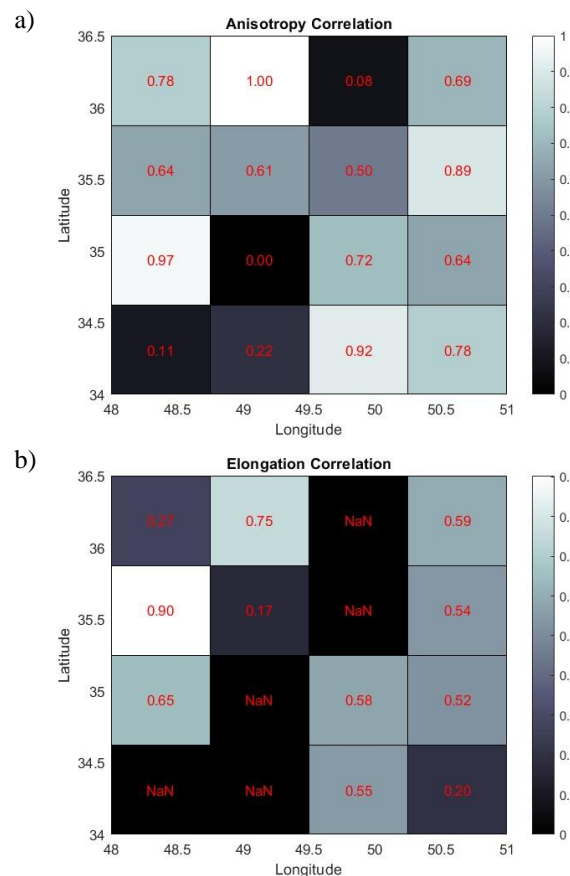


Figure 4. a) Anisotropic, and b) elongation correlation.

computed with distance lag of 5 arc-minute and azimuth lag of 22.5 arc-minute. Then the three ellipse parameters (i.e.,  $a$ ,  $b$ , and  $\theta$ ) for each patch are computed by simply fitting to the shape of empirical covariance in that patch.

To make comparison between gravity anomaly derived (Figure 2b) and laterally varying density covariances (Figure 3b) feasible, two types of correlation are defined; anisotropic and elongation correlation. By anisotropic correlation

$$C_{a_i} = 1 - \frac{|Az_{g_i} - Az_{d_i}|}{90}, \quad (15)$$

the similarity of the anisotropy angle is meant.  $Az_{g_i}$  and  $Az_{d_i}$  are azimuth of gravity anomaly and laterally varying density derived covariance of patch  $i$ . The elongation of each covariance ellipse is characterized by its axis ratio ( $a/b$ ). So, the elongation correlation in patch  $i$  is then defined as

$$C_{e_i} = \frac{a_{g_i}/b_{g_i}}{a_{d_i}/b_{d_i}}. \quad (16)$$

Figure 4a illustrate the anisotropic correlation between gravity anomaly and laterally varying density derived covariances of all patches. It shows that 11 patches have correlation more than 0.5. It means that in ~69% of the patches, gravity anomaly and laterally varying density derived covariances fall inside one quadrant of the circle. Elongation correlation of the patches are depicted in Figure 4b where 8 out of 11 patches with anisotropic correlation more than 0.5, have more than 0.5 elongation correlation too. In other word, by considering spatial-spectral correspondence of PLSC method, in half of the patches laterally varying density covariance could model the gravity anomaly derived covariances properly. To analysis elongation correlation, those patches that their anisotropic correlation are less than 0.5 (i.e., their Azimuth angle do not locate in the same quadrant) are ignored and filled out by NaN in Figure 4b. However, two patches on the south-western corner of R1 with anisotropic correlation of 0.00 and 0.11 has elongation near to  $(a/b) = 1$  (Figure 3b). When elongation of the covariance ellipse close to 1, the anisotropic determination becomes difficult.

#### 4. Discussion and Conclusion

This study pursued two main objectives. The first was to establish and review the formulation of Patch-wise LSC (PLSC). The PLSC approach integrates Moritz's step-wise LSC and multi-step LSC developed at Politecnico di Milano with the concept of spatial-spectral correspondence in gravity field signals as employed in RCR framework. According to this algorithm, the global and topography effect are removed from free-air corrected gravity anomaly observation up to degree and order  $N$ . Then the case study divided into  $t$  patches by area  $A$  and diameter  $\psi$  related to  $N$ . Next, patch-wise anisotropic covariances are determined based on available different functions and algorithms. After that, gravity field is modelled through LSC method. PLSC

is designed to mitigate the limitations of the stationarity assumption in LSC and to improve recovery of local, high-frequency gravity signals. By restricting covariance estimation to small spatial neighbourhoods, PLSC reduces the error arising from spatial heterogeneity and better captures local anisotropic behaviour.

In contrast, the point-wise non-stationary covariance approach of Darbeheshti (2009) considers the field to be fully non-stationary and anisotropic everywhere. However, practical implementation often results in abrupt changes in covariance parameters between adjacent points, compromising continuity and violating smoothness of the estimated field. As a result, this method must be constrained to a regular grid and requires the introduction of a tuning parameter  $\tau$  to stabilize parameter estimation. PLSC avoids these challenges: by assuming local stationarity and anisotropy within each patch, the auto- and cross-covariance matrices become block-diagonal, leading to significantly reduced computational cost relative to the point-wise approach.

The second objective of this work was to evaluate the localization performance implicit in PLSC. For this purpose, a global laterally varying density model (UNB\_TopoDensT\_2v01) was employed as an independent source of short-wavelength gravity variability at the patch scale. Patch-wise anisotropic covariance functions were derived for the R1 case study in north-western Iran by fitting elliptical models to empirical covariances computed from the UNB\_TopoDensT\_2v01 density anomalies. These density-derived covariances were compared with those obtained from residual gravity anomalies. Two similarity measures—anisotropic correlation and elongation correlation—were used to quantify the agreement between the two sources.

The results indicate that approximately 69% of the patches (11 out of 16) exhibit anisotropy directions that fall within the correct quadrant relative to the density-derived anisotropy. Among these, ~73% (8 out of 11 patches) show elongation correlations exceeding 50%. These findings demonstrate that the localization assumption embedded in PLSC is consistent—with more than 50% agreement—with the lateral density variations in the R1 region.

However, the accuracy and spatial resolution of global density models must also be considered. To enhance the reliability of this type of analysis, future work should incorporate local lateral density models derived from high-resolution geological maps or regional geophysical surveys. Moreover, vertically varying density and the relationship between spatial-spectral correspondence and depth-dependent mass distributions remain important factors that require additional investigation. Incorporating both laterally and vertically varying density models has the potential not only to refine covariance estimation from residual gravity anomalies but also to enable computation of density-derived anisotropic covariance functions in regions where gravity observations are sparse or unavailable.

## References

- Barthelmes, F. (2013). Definition of Functionals of the Geopotential and Their Calculation from Spherical Harmonic Models: Theory and formulas used by the calculation service of the International Centre for Global Earth Models (ICGEM). Scientific Technical Report STR 09/02, Revised Edition. Potsdam: Deutsches GeoForschungszentrum GFZ. <https://doi.org/10.2312/GFZ.b103-0902-26>.
- Darbeheshhti, N. & Featherstone, W., 2009. Non-stationary covariance function modelling in 2D least-squares collocation, *Journal of Geodesy*, 83(6), 495–508, <https://doi.org/10.1007/s00190-008-0267-0>.
- Farr, T.G., Rosen, P.A., Caro, E., Crippen, R., Duren, R., Hensley, S., Kobrick, M., Paller, M., Rodriguez, E., Roth, L., Seal, D., Shaffer, S., Shimada, J., Umland, J., Werner, M., Oskin, M., Burbank, D., Alsdorf, D. (2007). The shuttle radar topography mission. *Reviews of Geophysics* 45(2), <https://doi.org/10.1029/2005rg000183>.
- Forsberg, R., 1984. A study of terrain reductions, density anomalies and geophysical inversion methods in gravity field modelling, Department of Geodetic Science and Surveying, Ohio State University, Columbus.
- Förste, C., Bruinsma, S., Abrikosov, O., Lemoine, J., Schaller, T., Götze, H., Balmino, G. (2014). EIGEN-6C4, the latest combined global gravity field model including goce data up to degree and order 2190. GFZ Potsdam and GRGS Toulouse GFZ Data Services.
- Ghasemi, M., Ramouz, S., & Safari, A. (2023). On investigation of density correction and improved covariance effect on local modeling of gravity field by least squares collocation method in Iran. *Journal of the Earth and Space Physics*, 49(2), 371-388, <http://doi.org/10.22059/jesphys.2023.348002.1007454>
- Goad, C. C., Tscherning, C. C., & Chin, M. M., 1984. Gravity empirical covariance values for the continental united states, *Journal of Geophysical Research: Solid Earth*, 89(B9), 7962–7968, <https://doi:10.1029/JB089iB09p07962>.
- Hartmann, J., and N. Moosdorf (2012). The new global lithological map database GLiM: A representation of rock properties at the Earth surface. *Geochem. Geophys. Geosyst.*, 13,Q12004, <https://doi:10.1029/2012GC004370>.
- Higdon, D. (1998). A process-convolution approach to modelling temperatures in the North Atlantic Ocean. *Environmental and Ecological Statistics* 5(2), 173–190, <https://doi.org/10.1023/A:1009666805688>.
- Kamali, S., Safari, A., Ramouz, S., Reguzzoni, M., & Rossi, L., (under review). Covariance Estimation by Cross-validation in Local Gravity Field Modeling Using Patch-wise Least Squares Collocation, *Acta Geodaetica et Geophysica*.
- Moritz, H., 1980. *Advanced physical geodesy*, Wichmann.
- Paciorek, C. J. and M. J. Schervish 2006. Spatial modelling using a new class of nonstationary covariance functions. *Environmetrics* 17(5), 483-506, <https://doi.org/10.1002/env.785>.
- Ramouz, S., Afrasteh, Y., Reguzzoni, M., & Safari, A., 2020. Assessment of local covariance estimation through least squares collocation over Iran, *Advances in Geosciences*, 50, 65–75, <https://doi.org/10.5194/adgeo-50-65-2020>.
- Reguzzoni, M. & Tselfes, N., 2009. Optimal multi-step collocation: application to the space-wise approach for GOCE data analysis, *Journal of Geodesy*, 83(1), 13–29, <https://doi.org/10.1007/s00190-008-0225-x>.
- Sanso, F. & Sideris, M. G., 2013. *Geoid Determination: Theory and Methods*, Springer-Verlag, Berlin Heidelberg, <https://doi.org/10.1007/978-3-540-74700-0>.
- Sheng, M.-B., Shaw, C., Vaniček, P., Kingdon, R.W., Santos, M., & Foroughi, I. (2019). Formulation and validation of a global laterally varying topographical density model. *Tectonophysics*, 762, 45–60. <https://doi.org/10.1016/j.tecto.2019.04.005>.
- Tenzen, R., P. Sirguey, M. Rattenbury, J. Nicolson, (2011). A digital rock density map of New Zealand. *Computers & Geosciences*. Volume 37, Pages 1181-1191. <https://doi.org/10.1016/j.cageo.2010.07.010>
- Tscherning, C. C. & Rapp, R. H., 1974. Closed covariance expressions for gravity anomalies, geoid undulations, and deflections of the vertical implied by anomaly degree variance models, Report No. 208, Department of Geodetic Science, The Ohio State University, Columbus.